processes

MDPI

Article

Numerical Study on the Separation Performance of Hydrocyclones with Different Secondary Cylindrical Section Diameters

Duanxu Hou [1], Peikun Liu [1,*], Qiang Zhao [2], Lanyue Jiang [1], Baoyu Cui [3] and Dezhou Wei [3]

[1] College of Mechanical & Electronic Engineering, Shandong University of Science and Technology, Qingdao 266590, China; houduanxu@sdust.edu.cn (D.H.); jianglanyue5@sdust.edu.cn (L.J.)
[2] School of Metallurgy, Northeastern University, Shenyang 110819, China; zhaoqiang@mail.neu.edu.cn
[3] School of Resources & Civil Engineering, Northeastern University, Shenyang 110819, China
* Correspondence: lpk@sdust.edu.cn

Abstract: The particle motion behavior in hydrocyclones has received increasing attention, but the particle circulation flow has received relatively limited attention. In this paper, the particle circulation flow is regulated by changing the secondary-cylindrical section diameter to optimize the separation effect. The effects of secondary-cylindrical section diameters on flow field characteristics and separation performance are explored using the two-fluid model (TFM). The findings demonstrate that particle circulation flows are ubiquitous in the secondary-cylindrical hydrocyclone and are induced by the axial velocity wave zone. The increase in the secondary-cylindrical section diameter intensifies the coarse particle circulation and aggrandizes the coarse particle's aggregation degree and aggregation region, leading to an increment in cut size. The circulation flow component can be regulated by adjusting the secondary-cylindrical section, thus improving the classification effect. An appropriate diameter of the secondary-cylindrical section facilitates improved particle circulation, strengthening the separation sharpness.

Keywords: hydrocyclone; secondary-cylindrical section; particle circulation flow; separation performance

Citation: Hou, D.; Liu, P.; Zhao, Q.; Jiang, L.; Cui, B.; Wei, D. Numerical Study on the Separation Performance of Hydrocyclones with Different Secondary Cylindrical Section Diameters. *Processes* **2023**, *11*, 2542. https://doi.org/10.3390/pr11092542

Academic Editor: Monika Wawrzkiewicz

Received: 3 August 2023
Revised: 21 August 2023
Accepted: 22 August 2023
Published: 25 August 2023

1. Introduction

The hydrocyclone is an active equipment that utilizes centrifugal force to achieve accelerated separation [1,2]. It is widely used in minerals, chemicals, petroleum engineering, environmental protection, food processing, and papermaking. Hydrocyclones have the advantages of having no moving parts, being simple to operate, having a large processing capacity, and being easy to maintain compared to other separation devices [3,4]. Despite these advantages, the separation efficiency and the cut sharpness are limited by complex interphase interaction and strong turbulence [5,6].

The particle movement characteristics in the hydrocyclone decide the spatial distribution of the hydrocyclone affecting the separation effect. Researchers have extensively researched particle motion behavior and its regulatory mechanism to improve the separation effect. Zhang [7] discovered that under high-concentration feeding conditions, fine particles with a higher density are easily misplaced in the underflow. In contrast, coarse particles with a smaller particle size were more likely to be misplaced in the overflow. Hao [8] found that particles near the wall rotate at a high rate, causing particles to gravitate toward the center. Yang [9] found that the particle arrangement at the inlet affected the separation effect remarkably, thus designing a particle arrangement unit. Wang [10] believed that the inlet with a pre-sedimentation function is very helpful for the separation. Fu [11] discovered that a smaller cone angle can increase particle revolution and self-rotation speeds while decreasing average particle residence time. Zhang [12] discovered that a

tangent-circle inlet could improve the radial regular distribution of particles and alleviate particle misplacement. According to Li [13], a curved inlet facilitates coarse particles moving toward the wall and fine particles moving toward the air core.

The separation effects are associated with circulation flow within hydrocyclone. It is critical for further understanding the hydrocyclone separation mechanism by studying the internal circulation flow, particularly the particle circulation in the separation chamber. Kelsall [14] was the first to discover circulation flow in the upper cylindrical section, which increases particle residence time. He et al. [15] found the circulation flow in the underside region of a micro hydrocyclone by phase Doppler particle analyzer (PDPA). Hwang et al. [16] discovered that the cone-shaped top plate could reduce the lower velocity surrounding the vortex finder, thereby reducing the circulation of fine particles. Zhao [17] pointed out that the thick-walled vortex finder eliminates the circulation flow surrounding the vortex finder while creating circulation flow in the axial velocity wave zone (AVWZ). Jiang et al. pointed out that an arc-shaped vortex finder can suppress circulation flow around the vortex finder [18]. Hsu et al. [19] believed that the strong circulation flow around the vortex finder causes the unseparated particles to escape directly from the vortex finder. Liu et al. [20] believed that the velocity gradient between adjacent flow layers is the primary cause of circulation flow and regarded the flow rate as the flow in the AVWZ. Unfortunately, most of these studies focus on analyzing the effect of water circulation on particle separation behavior using qualitative or quantitative methods, but few studies are devoted to particle circulation in hydrocyclones.

Recently, several sophisticated measurement techniques have been employed in investigating the flow field and particle motion properties of hydrocyclones [21–25]. He et al. [15] and Liu et al. [20] studied the internal circulation flow of hydrocyclones by the PDPA. However, the representativeness of test results under high concentration conditions makes it difficult to apply these advanced measurement techniques to study particle circulation in hydrocyclones. The advancement of highly performant computing technology and computational fluid dynamics (CFD) has made it possible to explore particle circulation flow in hydrocyclones. The widely used numerical methods are categorized into the Eulerian-Lagrange and Eulerian-Eulerian models [26–28]. Owing to ignoring the inter-particle interaction, the Eulerian-Lagrange model is mostly used in dilute phase regimes [29–31]. The emergence of the Dense Discrete Phase model (DDPM) overcomes the inherent defects of the Eulerian-Eulerian model, but the large calculation amount makes investigating particle circulation in hydrocyclones more difficult [32–34]. For the Eulerian-Eulerian, all phases are considered as a continuous medium, and the interaction between particles is calculated by the kinetic theory of granular flow (KTGF) [6,35,36]. Because of its high computational efficiency and reliable numerical results, the Eulerian-Eulerian model is extensively applied to investigate the separation process of hydrocyclones [36–38].

This paper explains links between the AVWZ, particle circulation flow and separation effect, varying the secondary-cylindrical section diameters. The flow field in different hydrocyclones is studied by a verified TFM model to clarify the particle circulation flow. Then, the mechanism underlying the correlation between particle circulation flow and separation performance is explored by examining the particle circulation flow, AVWZ, particle spatial distribution, and separation effect. This research is anticipated to better understand the relations between the particle circulation flow and the separation performance of hydrocyclones and provide a guide for the design and optimization of the hydrocyclone.

2. Simulation Method and Conditions

2.1. Model Description

Considering the complicatedness of the flow field in hydrocyclones, the simulation process is divided into two stages to guarantee the stabilization of the numerical models. Firstly, the air-water two-phase flow field was calculated using the TFM to obtain the flow field characteristics of the hydrocyclone with different secondary cylindrical sections. Then, the air-water-solid three-phase flow field is calculated to acquire the circulation particle

flow and separation efficiency. The turbulent flow in the hydrocyclone is calculated using the Reynolds stress model (RSM), which can model the turbulent anisotropy problem at a less computationally expensive than the large eddy simulation (LES) model [39–41]. A detailed description is provided in the Supplementary File.

2.2. Simulation Conditions

To study particle circulation flow's impact on the separation property, eight hydrocyclones with different structures were designed to control particle circulation flow by changing secondary-cylindrical section diameters. The secondary-cylindrical hydrocyclone, also known as cylindrical-conical-cylindrical (CCC) hydrocyclone, and its design ideas can be found elsewhere [42]. The geometric parameters and computational domain grid of hydrocyclones with various structures are presented in Figures 1 and 2, respectively. To capture the minor variations in the flow field, the mesh around the wall, vortex finder, spigot, and the bottom of the secondary-cylindrical section are refined. The results of grid independence show that the grid scheme used in this paper is grid independent and converged. Detailed information is provided in the Supplementary File.

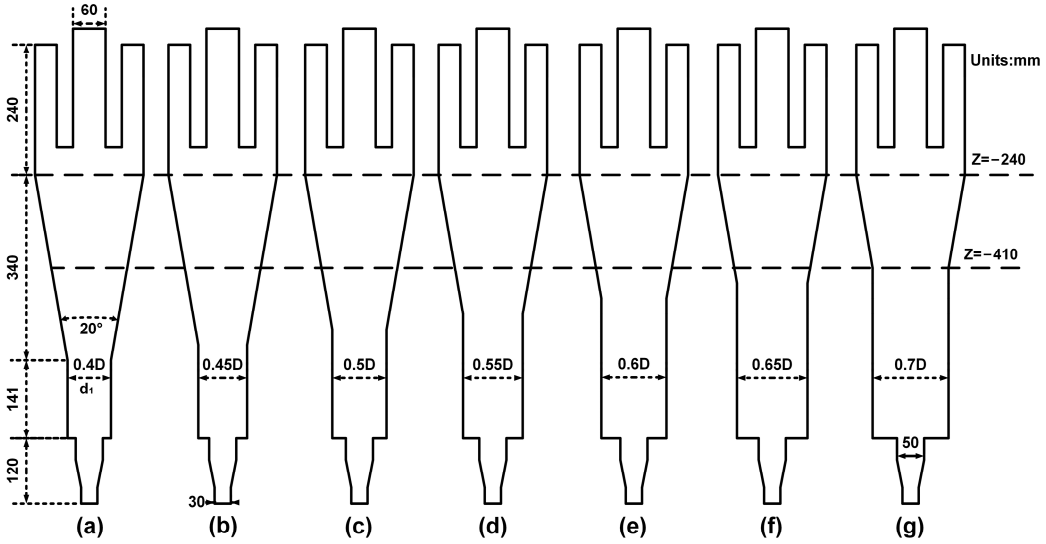

Figure 1. Geometric parameters of hydrocyclones: (**a**) D_1 = 0.4D; (**b**) D_1 = 0.45D; (**c**) D_1 = 0.5D; (**d**) D_1 = 0.55D; (**e**) D_1 = 0.6D; (**f**) D_1 = 0.65D; (**g**) D_1 = 0.7D.

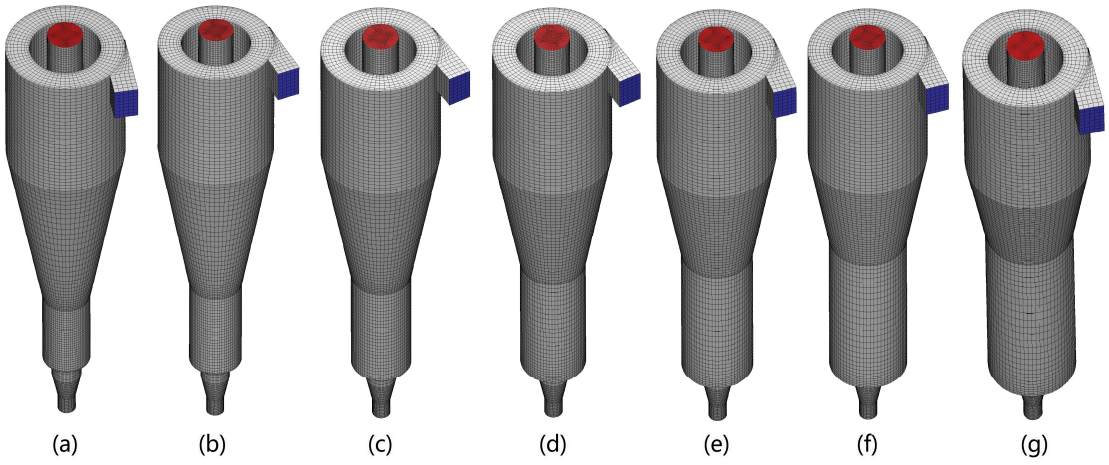

Figure 2. Domain mesh of hydrocyclones: (**a**) D_1 = 0.4D; (**b**) D_1 = 0.45D; (**c**) D_1 = 0.5D; (**d**) D_1 = 0.55D; (**e**) D_1 = 0.6D; (**f**) D_1 = 0.65D; (**g**) D_1 = 0.7D.

Boundary conditions for the inlet are "velocity inlet" with a fixed velocity of 3 m/s for water and solids, and the solid phase released from the inlet is determined by physical experiments to be in a volume fraction of 16.86%. A "pressure outlet" boundary condition is applied to both the overflow and underflow, while the outlet pressure is assumed to be 1 atmosphere and the backflow volume fraction of air is assumed to be 1. The wall boundary conditions of air and water are non-slip, while the specular coefficient of 0.6 is used for particles [43,44]. The solid particles used in this paper are quartz samples, and the particle size composition is presented in the Supplementary File.

2.3. Model Applicability

The validation is essential to verify the reliability of the numerical models before using them for numerical tests. The air-water two-phase and air-water-solid three-phase flow models are verified according to the Laser Doppler Velocimetry (LDV) and physical separation experiment results, respectively. Overall, all numerical models used in the present study can accurately predict the flow field characteristics and separation performance of the cylindrical hydrocyclone, as described in the Supplementary File.

3. Results and Discussion

3.1. Flow Fields

3.1.1. Particle Flow Fields

The particle flow field is analyzed to analyze the particle circulation flow and particle movement behavior. For simplicity, only three representative particles of 10 μm (fine particle), 59.5 μm (medium particle), and 150 μm (coarse particle) are studied, as illustrated in Figure 3.

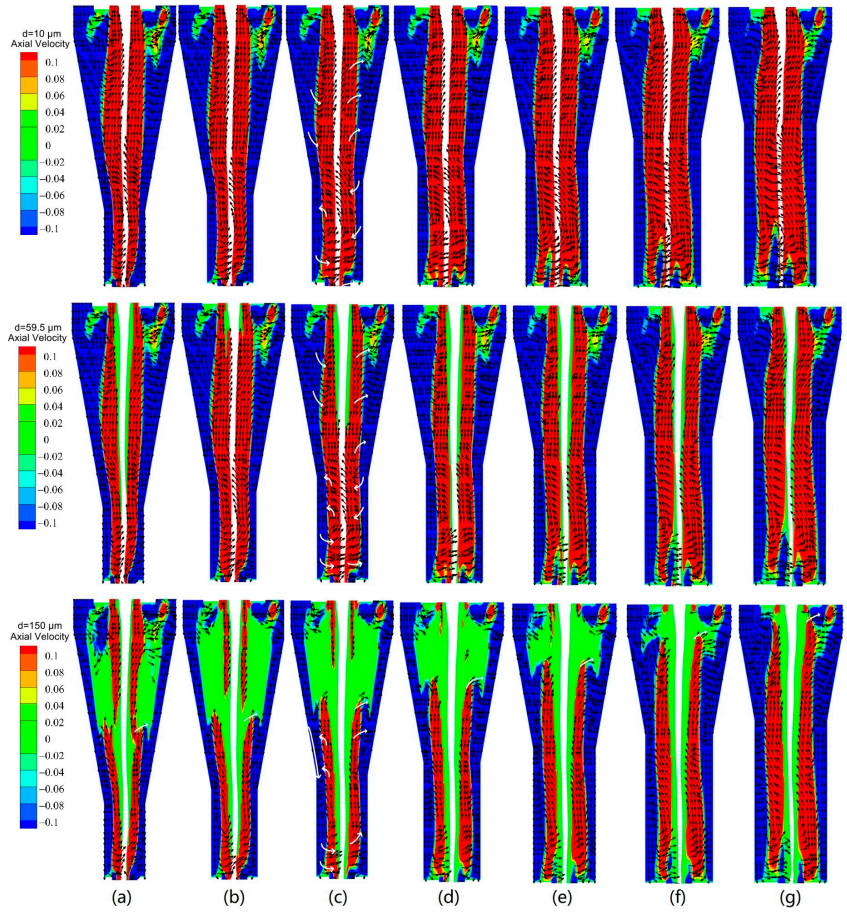

Figure 3. Effect of the secondary-cylindrical section on the particle flow field: (**a**) D_1 = 0.4D; (**b**) D_1 = 0.45D; (**c**) D_1 = 0.5D; (**d**) D_1 = 0.55D; (**e**) D_1 = 0.6D; (**f**) D_1 = 0.65D; (**g**) D_1 = 0.7D.

Fine particle and medium particle circulation flow in hydrocyclones are ubiquitous. Taking the hydrocyclone of D_1 = 0.5D as an example, the fine particles and medium particles travel towards the central and change into the internal swirling flow under the drag force, while part of the fine and medium particles move toward the wall under the centrifugal force during moving with the internal swirling flow, as shown by the white arrow in Figure 3. Simultaneously, the particle entering the internal swirling flow from the external swirling flow and the particle entering the external swirling flow from the internal swirling flow is coexistence instead of single at certain axial sections. Hence, abundant particle circulating flows are formed within the hydrocyclone. At the bottom of the secondary-cylindrical section, fine particles and medium particles have to cross the internal swirling flow region while moving toward the underflow, increasing the probability of moving with the internal swirling flow and reducing fine particle misplacement in the underflow.

Different from fine and medium particles, coarse particles travel along the wall to the bottom of the hydrocyclone. However, some coarse particles are entrained by the internal swirling flow during travel toward the spigot and move upward. The coarse particles moving with the internal swirling flow gradually move towards the wall and return to the external swirling flow region under the centrifugal force, forming the particle circulating flow. The coarse particle circulation region expands as the secondary-cylindrical section diameter increases, implying an increase in the coarse particle circulation flow. Meanwhile, the coarse particles circulation flow zone shifts towards the underside of the vortex detector by increasing the secondary-cylindrical section diameter, potentially exacerbating the misplacement phenomenon of coarse particles.

3.1.2. AVWZ

The AVWZ is the source of particle circulation flow in hydrocyclone, which directly affects the separation performance [20,30]. As a result, the AVWZ in various hydrocyclones is investigated to understand particle circulation flow better, and the results are shown in Figure 4. Since there is no definitive description of the AVWZ in the previous publications, the AVWZ is considered the region with the magnitude of axial velocity less than axial fluctuation velocity based on the low and fluctuating characteristics of axial velocity in AVWZ, and the red zone in Figure 4 represents the AVWZ.

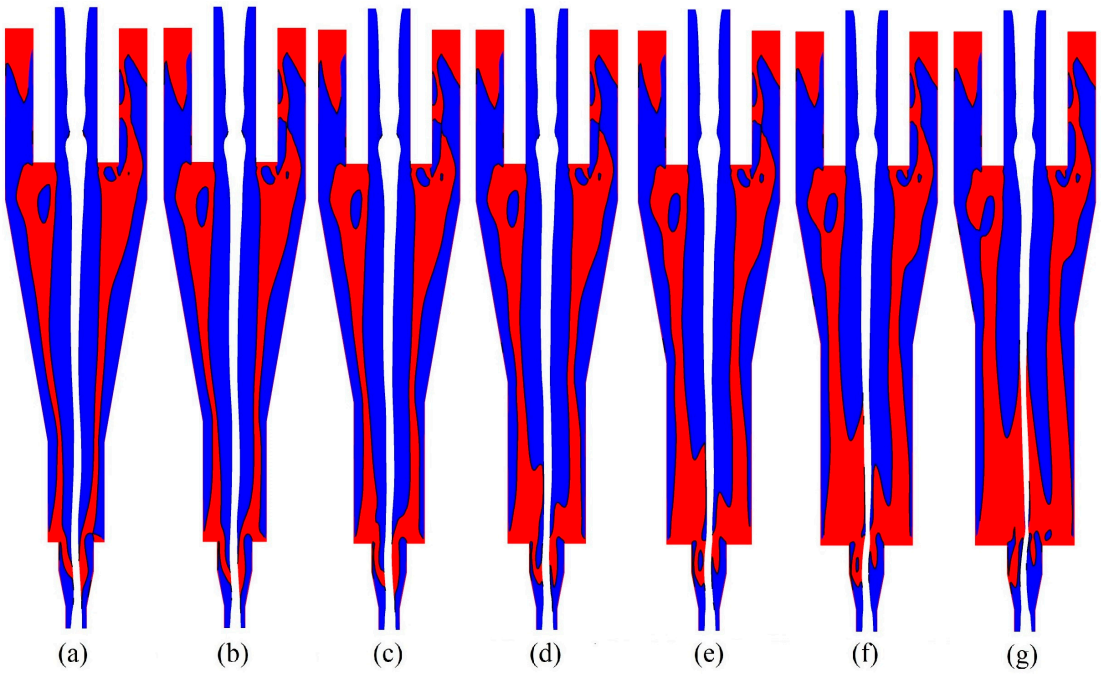

Figure 4. Effect of the secondary-cylindrical section on the AVWZ: (**a**) D_1 = 0.4D; (**b**) D_1 = 0.45D; (**c**) D_1 = 0.5D; (**d**) D_1 = 0.55D; (**e**) D_1 = 0.6D; (**f**) D_1 = 0.65D; (**g**) D_1 = 0.7D.

The increase in secondary-cylindrical section diameter enlarges the AVWZ, especially at the bottom of the secondary-cylindrical section, which can be attributed to the expansion in the flat-bottomed structure diameter of cylindrical-conical-cylindrical hydrocyclone. For the secondary-cylindrical section with a large diameter, the bottom region is dominated by the AVWZ, resulting in more particle circulation flow affected by AVWZ during particle moving to the spigot, which further explains the increase in the upward flow ratio and downward flow ratio of medium particle and coarse particle. The AVWZ at the bottom of the secondary-cylindrical section facilitates fine particles trapped by coarse particles returning to the separating zone, thus decreasing the misplacement of fine particles. However, the abundant AVWZ accelerates the coarse particles that have been separated to return to the separation region again, which may restrict the processing capacity and increase the misplacement of coarse particles. A minor increase in the amplitude of AVWZ in the middle and upper part of the hydrocyclone can be used to explain the limited effect of the secondary-cylindrical section diameter on the upward flow ratio and downward flow ratio of fine particles.

3.2. Particle Circulation Flow

3.2.1. Downward Flow Ratio

Figure 5 depicts the impact of the secondary-cylindrical section on the particle downward flow ratio. For simplicity, only three characteristic particles of 10 μm (fine particles), 59.5 μm (medium particles), and 150 μm (coarse particles) are evaluated. The calculation of the downward flow ratio can be found in the Supplementary File.

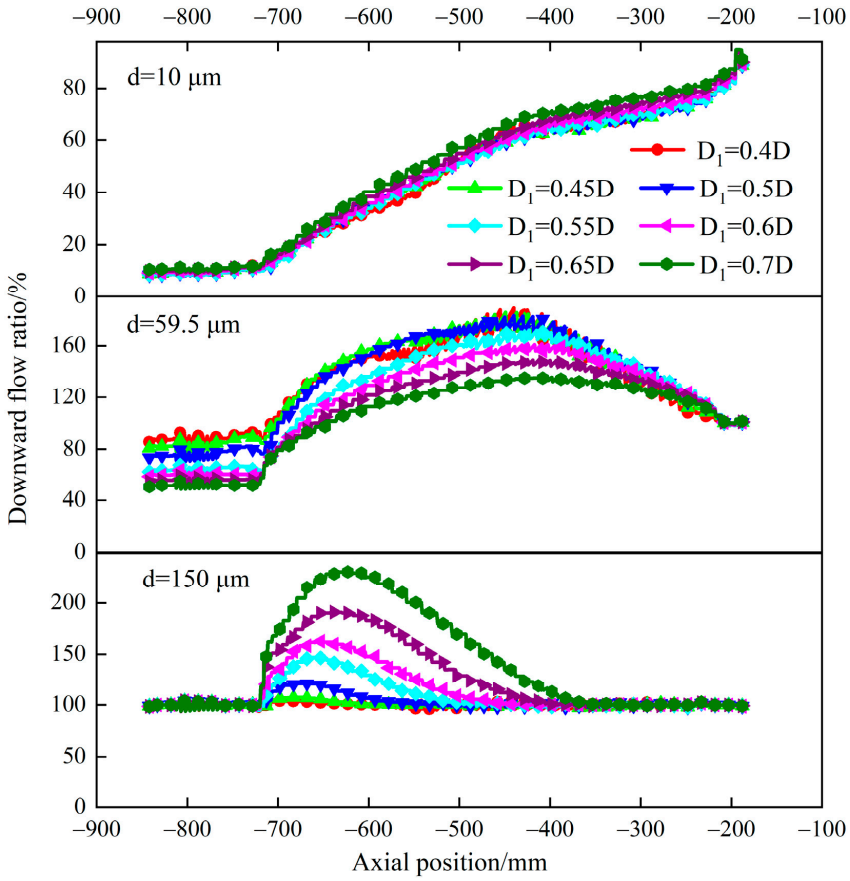

Figure 5. Effect of the secondary-cylindrical section on particles downward flow ratio.

For 10 μm particles, the downward flow ratio in different hydrocyclones decreases by reducing the axial position caused by drag force. However, the particle downward flow ratio around the Z = −300 mm section has a tiny variation, which could be explained

by the relative balance of particles passing into the internal swirling flow with particles entering back into the external swirling flow caused by the circulation flow. Simultaneously, the secondary-cylindrical section diameter slightly affects the fine particle downward flow ratio.

For 59.5 μm particles, the downward flow ratio in different hydrocyclones increases first and decreases with decreasing axial position. Due to the circulation flow at the upper portion of hydrocyclones, particle movement is dominated by returning from the interior swirling flow to the exterior swirling flow, increasing the particle downward flow ratio. While a large number of particles are coerced by interior swirling flow at the inferior portion of the hydrocyclone, decreasing the particle downward flow ratio. Concurrently, the downward flow ratio of 59.5 μm particle reduces with increasing the secondary-cylindrical section diameter at the same axial section, implying a reduction in the circulation flow of 59.5 μm particle.

In different hydrocyclones, the downward flow ratio of 150 μm particle firstly increased and then reduced with decreasing axial positions, owing to particle circulation flow and interior swirling flow, respectively. With increasing the secondary-cylindrical section diameter, the circulation flow region and the downward flow ratio of 150 μm particles increase, consistent with the findings in Figure 3. Meanwhile, the downward flow ratio of 150 μm particles is significantly greater compared to the inlet flow ratio, indicating abundant particle circulation flow in hydrocyclones, but more coarse particles circulating in the hydrocyclone result in the misplacement of coarse particles [32].

3.2.2. Upward Flow Ratio

The impact of the secondary-cylindrical section on the upward flow ratio is illustrated in Figure 6. The calculation of the upward flow ratio can be found in the Supplementary File.

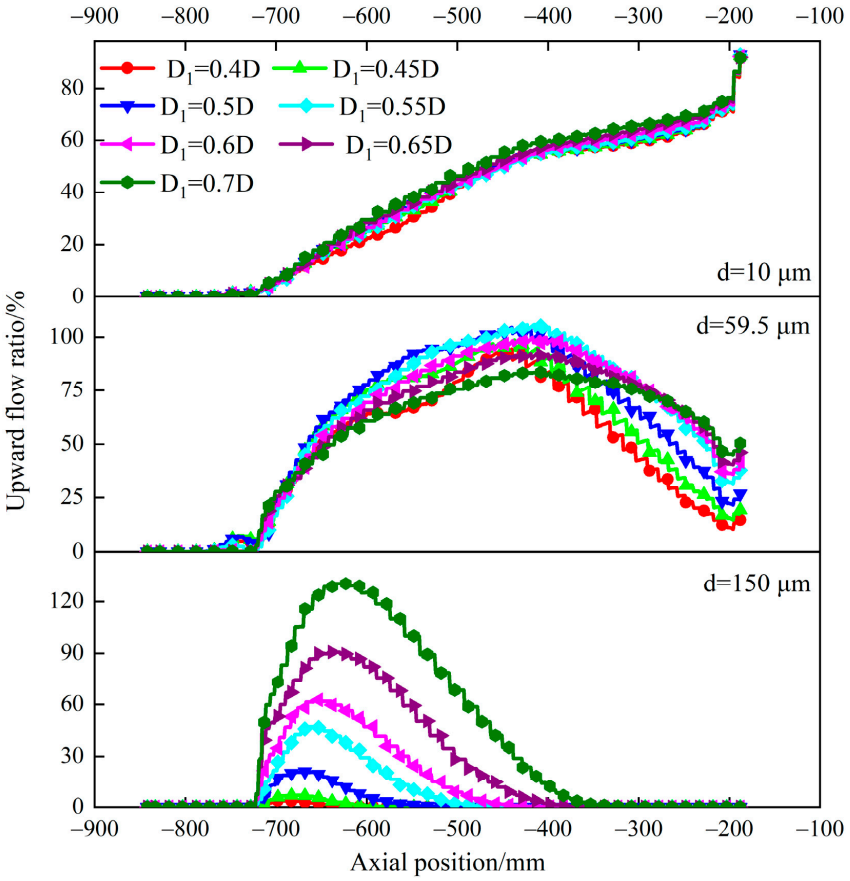

Figure 6. Effect of the secondary-cylindrical section on particles upward flow ratio.

The variation of the particle upward flow ratio with axial position is consistent with that of the downward flow ratio. For fine particles (d = 10 μm), particles into the internal flow are larger than those into the external flow at different axial sections, and the upward flow ratio of 10 μm particles increases as the axial position increases. On the other hand, the gently varying region of the upward flow near the Z = −300 mm section demonstrates that particles entering and exiting the internal swirling flow region have reached a dynamic balance. The secondary-cylindrical section diameter slightly affects the upward flow ratio of fine particles, which is consistent with the downward flow ratio, implying that the secondary-cylindrical section diameter affects the circulating flow of fine particles lightly.

For 59.5 μm particles, the upward flow ratio increases first and then decreases as the axial position increases. In some axial sections, the particle upward flow ratio exceeds 100%, indicating a particle circulation flow in hydrocyclones. The upward flow ratio of 59.5 μm particles in the middle of the hydrocyclone increases first and then decreases with the increase of secondary-cylindrical section diameter. However, the increase of secondary-cylindrical section diameter increases the upward flow ratio of 59.5 μm particles underneath the vortex finder, implying more particles discharged with the overflow, which may contribute to increasing the cut size.

For 150 μm particles, the upward flow ratio is approximately 0 nearby the vortex finder of different hydrocyclones. Essentially, no coarse particles move with the internal swirling flow, indicating no significant misplacement of the coarse particle in the overflow. However, the particle upward flow ratio in other positions of the hydrocyclone increase with secondary-cylindrical section diameter, and the particle upward flow ratio in part of the axial sections exceeds the inlet flow rate, demonstrating the ubiquity of particle circulation flow. On the other hand, the large secondary-cylindrical section diameter expands the region with coarse particle upward flow, thereby expanding the coarse particle circulation flow region. In general, the effect of the secondary-cylindrical section diameter on the upward and downward flow ratios of 150 μm particles is stronger than that on fine particles, implying that the secondary-cylindrical section has a greater effect on the coarse particle circulation flow.

3.2.3. Circulation Flow Ratio and Circulation Flow Proportion

The particle circulation flow ratio in hydrocyclones with different secondary-cylindrical sections is presented in Figure 7. The particle circulation flow ratio calculation can be found in the Supplementary File.

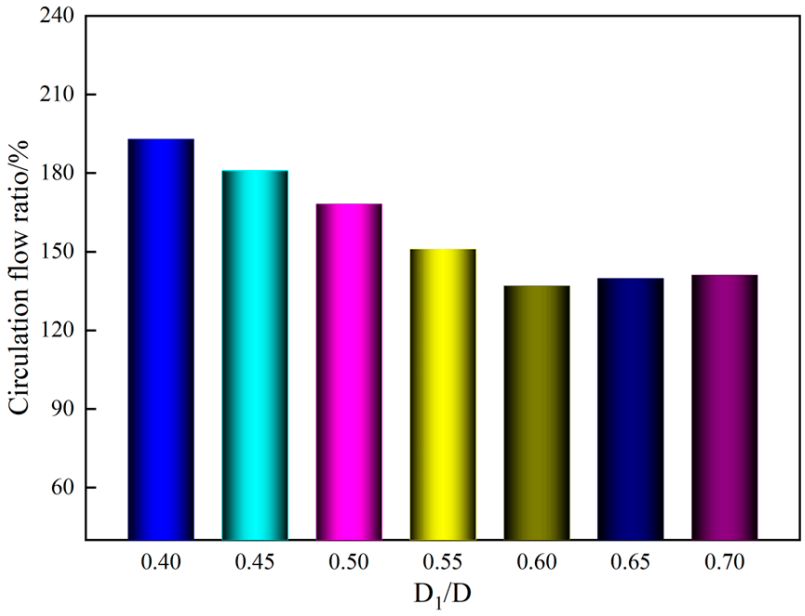

Figure 7. Effect of the secondary-cylindrical section on circulation flow ratio.

It can be detected that the circulation flow ratio in different hydrocyclone is greater than 100%, further indicating a substantial particle circulation flow in hydrocyclones, which agrees with the outcomes of Figures 5 and 6. Moreover, the particle circulation flow ratio tends to decrease and then increase slightly with the increases of the secondary-cylindrical section diameter and reaches the minimum value at 0.6D. The enhancement of the coarse particle circulation flow hinders the centrifugal settling process of particles, which in turn inhibits the development of the particle circulation flow, thus decreasing the circulation flow ratio. However, a further increase in the particle circulation flow ratio is induced with a sufficiently strong coarse particle circulation flow.

The fine particles (10 μm and 29 μm) circulation flow proportion ($R_{C,f}$), medium particles' (41.5 μm, 59.5 μm, and 89 μm) circulation flow proportion ($R_{C,m}$), and coarse particles (127 μm and 150 μm) circulation flow proportion ($R_{C,c}$) are investigated to analyze further the particle circulating flow composition. The outcomes are presented in Figure 8. The calculation of the particle circulation flow proportion can be found in the Supplementary File.

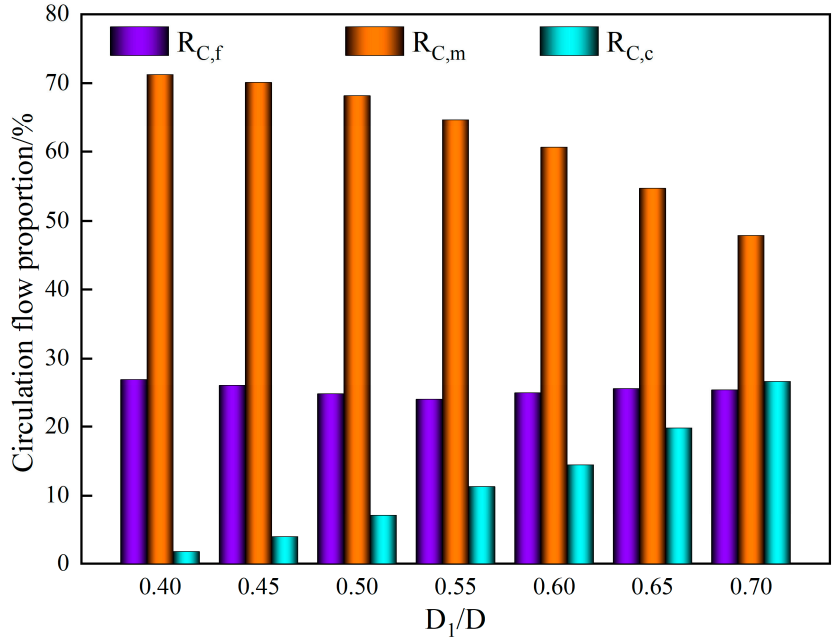

Figure 8. Effect of the secondary-cylindrical section on circulation flow proportion.

The medium particle circulation is dominant I in hydrocyclones with different secondary-cylindrical sections. The medium particle circulation flow proportion decreases monotonically with increasing the secondary-cylindrical section diameter, while the coarse particle circulation flow proportion increases monotonically. Accordingly, an increase in the secondary-cylindrical section diameter can intensify the coarse particle circulation flow and attenuate the medium particle circulation flow, potentially contributing to a greater cut size. Consequently, the composition of the particle circulation flow can be regulated by altering the secondary-cylindrical section to purposefully strengthen or attenuate the specific particle circulation flow, thus improving the separation performance. However, the fine particle circulation proportion is independent of the secondary-cylindrical section, which could be attributed to the fact that the fine particle circulation flow is concentrated in the middle and upper regions of hydrocyclones, while there is no obvious fine particle circulation flow in the secondary-cylindrical section.

3.3. Particle Spatial Distribution

The particle movement behavior determines its spatial distribution and separation behavior. The particle distribution in various hydrocyclones is investigated to analyze

the impact of particle circulation flows on it. For simplicity, the spatial distribution of the particle phase and three representative particles are characterized, and the findings are displayed in Figures 9–12.

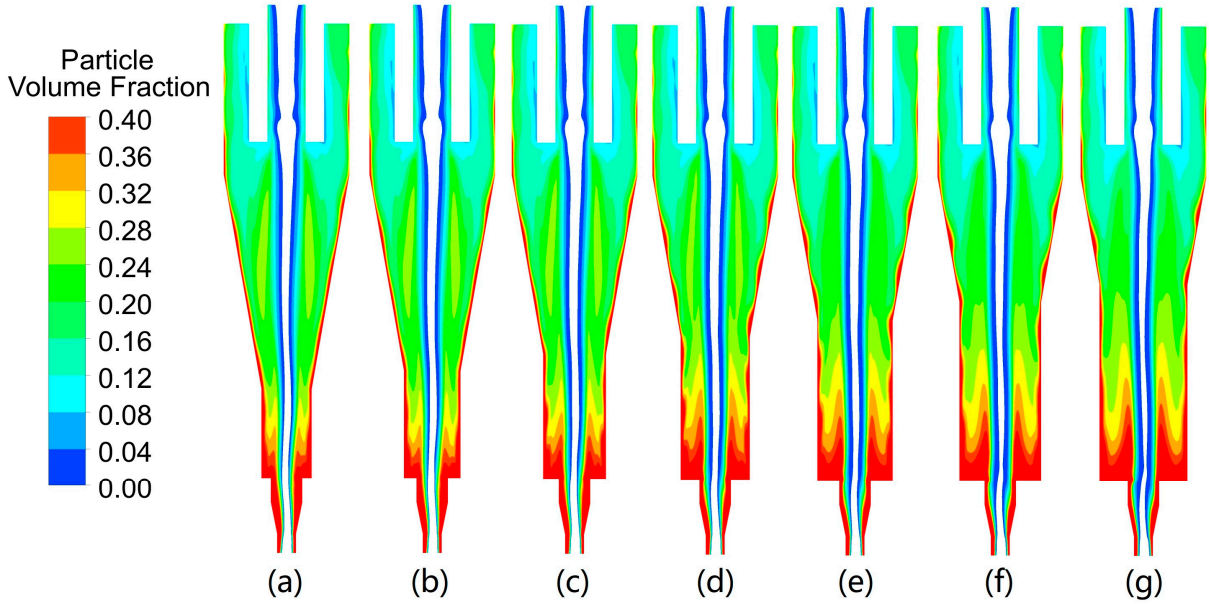

Figure 9. Effect of the secondary-cylindrical section on particle volume fraction: (**a**) D_1 = 0.4D; (**b**) D_1 = 0.45D; (**c**) D_1 = 0.5D; (**d**) D_1 = 0.55D; (**e**) D_1 = 0.6D; (**f**) D_1 = 0.65D; (**g**) D_1 = 0.7D.

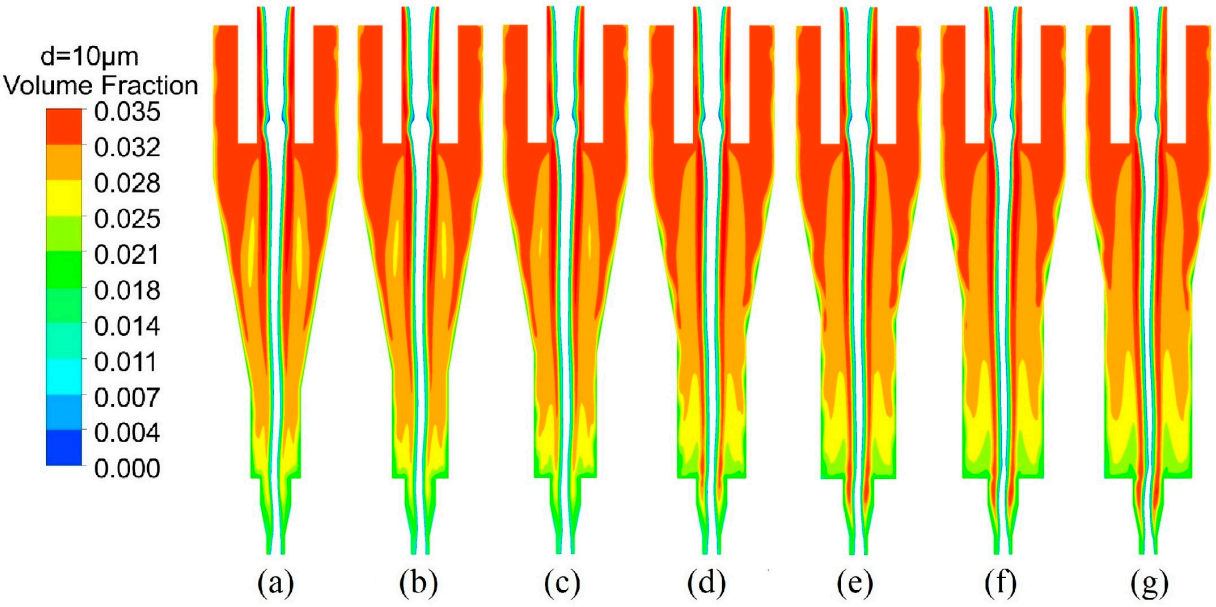

Figure 10. Effect of the secondary-cylindrical section on the particle volume fraction of d = 10 μm: (**a**) D_1 = 0.4D; (**b**) D_1 = 0.45D; (**c**) D_1 = 0.5D; (**d**) D_1 = 0.55D; (**e**) D_1 = 0.6D; (**f**) D_1 = 0.65D; (**g**) D_1 = 0.7D.

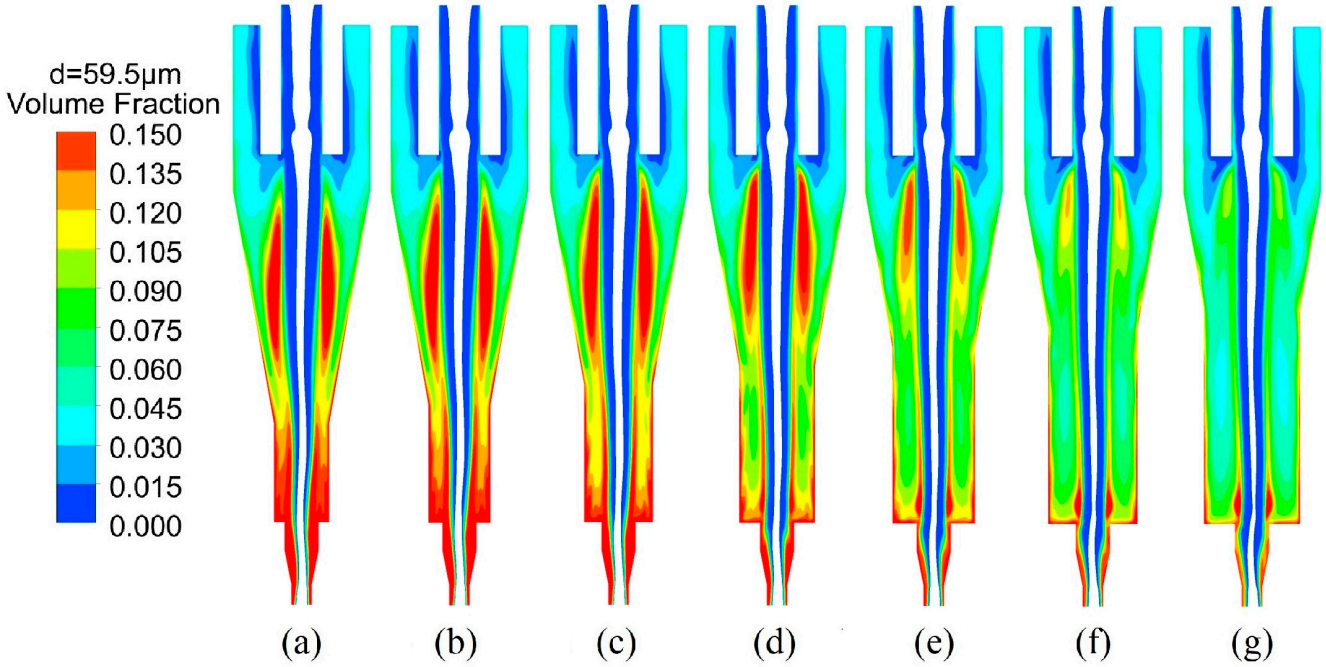

Figure 11. Effect of the secondary-cylindrical section on the particle volume fraction of d = 59.5 μm: (**a**) D_1 = 0.4D; (**b**) D_1 = 0.45D; (**c**) D_1 = 0.5D; (**d**) D_1 = 0.55D; (**e**) D_1 = 0.6D; (**f**) D_1 = 0.65D; (**g**) D_1 = 0.7D.

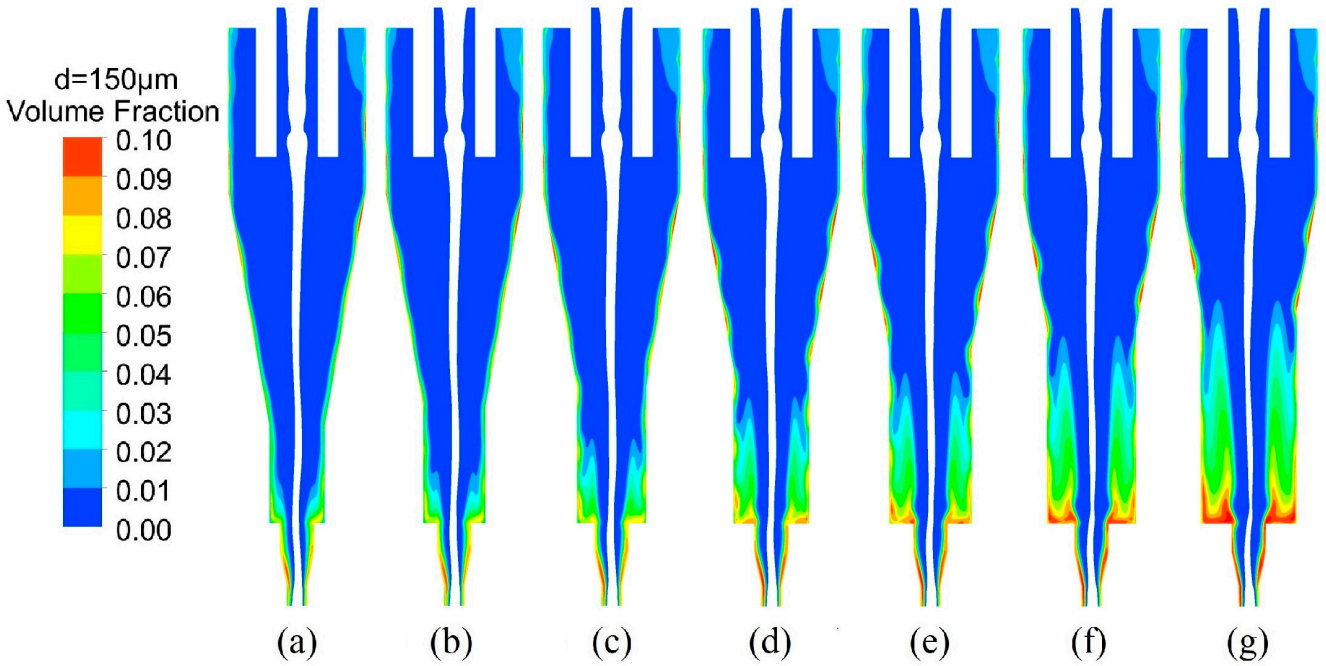

Figure 12. Effect of the secondary-cylindrical section on the particle volume fraction of d = 150 μm: (**a**) D_1 = 0.4D; (**b**) D_1 = 0.45D; (**c**) D_1 = 0.5D; (**d**) D_1 = 0.55D; (**e**) D_1 = 0.6D; (**f**) D_1 = 0.65D; (**g**) D_1 = 0.7D.

The particle phase in various hydrocyclones aggregates at the bottom of the secondary-cylindrical section resulting in a dense regime, and the dense regime region expands as the secondary-cylindrical section diameter increases. Because the axial velocity is low and fluctuating, particle movement efficiency in the AVWZ is reduced, resulting in particle aggregation. The strong particle-particle interaction in the dense regime region, on the other hand, prevents particles from moving through the dense regime to the spigot, which increases the extent of particle aggregation. Due to the inability to discharge from the

underflow in time, the possibility of particles in the dense regime forming circulation flow is enlarged. Concurrently, the secondary-cylindrical section diameter slightly impacts the volume fraction distribution of the particle phase in the top section of hydrocyclones.

Figure 10 depicts the effect of secondary-cylindrical section diameter on the spatial distribution of 10 μm particles. The secondary-cylindrical section diameter slightly affects the spatial distribution of 10 μm particles, which can be attributed to the slight difference in fine particle circulation flow of different hydrocyclones. The increase in the secondary-cylindrical section diameter reduces the volume fraction of 10 μm particles at the bottom of the hydrocyclone, which may contribute to reducing fine particle circulation flow and misplaced fine particles in the underflow. The volume fraction of 10 μm particles increases slightly by increasing the secondary-cylindrical section diameter in the upper part of the hydrocyclone, which helps the fine particles to be discharged quickly with the overflow.

The secondary-cylindrical section diameter significantly affects the spatial distribution of 59.5 μm particles, illustrated in Figure 11. In the lower part of hydrocyclones, the aggregation extent of 59.5 μm particles is reduced as the secondary-cylindrical section diameter increases caused by the reduction in the particle downward flow ratio. The smaller volume fraction in the AVWZ reduces particle circulation flow, resulting in a decrease in particle upward flow ratio. However, the volume fraction of 59.5 μm particles increases first and then decreases by increasing the secondary-cylindrical section diameter underneath the vortex finder, reaching the maximum when D_1 = 0.5D. The increase of particle aggregation extent under the vortex finder may be ascribed to an increase in particle upward flow ratio. However, the lower circulation flow of 59.5 μm particles reduces the particle upward flow ratio and particle downward flow ratio in the hydrocyclone with a large secondary-cylindrical section diameter. Then it reduces the concentration of 59.5 μm particles.

The impact of the secondary-cylindrical section on the spatial distribution of 150 μm particle is depicted in Figure 12. At the bottom of hydrocyclones, the volume fraction of 150 μm particle increases with the increase of the secondary-cylindrical section diameter caused by a larger AVWZ. Synchronously, the larger particle upward flow ratio in the hydrocyclone with an expanded secondary-cylindrical section aggravates the aggregation region of 150 μm particles to spread towards the vortex finder. The above analysis further proves that the coarse particle circulation flow region increases as the secondary-cylindrical section diameter increases. On the other hand, there is no obvious aggregation of 150 μm particles under the vortex finder in the hydrocyclone of D_1 = 0.7D, which may imply that the large secondary-cylindrical section diameter strengthens the coarse particle circulation flow but does not aggravate misplaced coarse particles in the overflow. The preceding analyses suggest that particle circulation flow is one of the principal reasons for particle aggregation in hydrocyclones.

3.4. Particles Separation Performance

The effect of the secondary-cylindrical section diameter on the separation efficiency is depicted in Figure 13. The separation efficiency curve is categorized into three zones: fine particle zones (d < 30 μm), coarse particle zones (d > 100 μm), and medium particle region (30 μm $\leq$ d $\leq$ 100 μm).

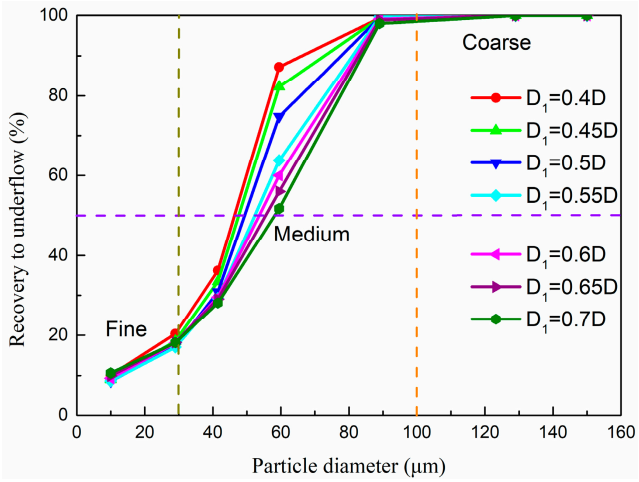

Figure 13. Effect of the secondary-cylindrical section on the separation efficiency of hydrocyclones.

Compared with fine and coarse particles, the secondary-cylindrical section diameter affects the medium particle separation efficiency to a greater extent. The larger secondary-cylindrical section diameter decreases the medium particle separation efficiency, implying more medium particles discharged with the overflow. Since the secondary-cylindrical section diameter affects the movement behavior of fine particles in a negligible way, no significant difference in the fine particle separation efficiency can be observed. Notwithstanding, the secondary-cylindrical section strengthens the coarse particle circulation flow and expands the coarse particle aggregation region. However, the coarse particles moving with the internal swirling flow will return to the external swirling flow region and eventually be discharged with the underflow caused by the centrifugal force. Hence, the difference in coarse particle separation efficiency between hydrocyclones is minor.

The impact of the secondary-cylindrical section on the cut size (d_{50}) and imperfection value (I) is depicted in Figure 14. The cut size increases monotonically by increasing the secondary-cylindrical section diameter caused by the exaggerated AVWZ. Consequently, hydrocyclones with a larger secondary-cylindrical section diameter can improve cut size while reducing misplaced coarse and fine particles, which is advantageous for operations requiring a larger cut size. A minor imperfection value indicates superior separation sharpness and more satisfactory separation results. The imperfection value reduces and then enlarges as the secondary-cylindrical section diameter increases. When D_1 = 0.5D, the imperfection value achieves a minimized value of 0.23. In summary, the separation sharpness of the hydrocyclone could be enhanced by enlarging the secondary-cylindrical section diameter.

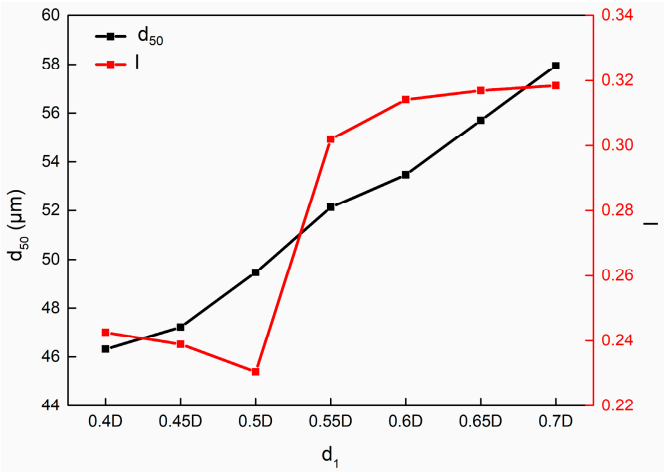

Figure 14. Effect of the secondary-cylindrical section on the cut size and imperfection value.

4. Conclusions

The impact of particle circulation flow on the separation performance of hydrocyclones was investigated by adjusting the secondary-cylindrical section diameter. The main findings are concluded in the following:

1. Particle circulation flow is ubiquitous in hydrocyclones, and the region of particle circulation flow expands with increasing the secondary-cylindrical section diameter.
2. The upward flow ratio and downward flow ratio of fine particles decrease as the axial position decreases, whereas the upward and downward flow ratio of medium particles and coarse particles increase and then decrease. A larger secondary-cylindrical section diameter can enhance the coarse particle circulation flow and suppress the medium particle circulation flow, thus reducing the particle circulation flow ratio.
3. The impact of secondary-cylindrical section diameter on the fine particle circulation flow is negligible, whereas superior AVWZ in hydrocyclones of large secondary-cylindrical section diameter augments coarse particles circulation flow, increasing the aggregation extent and aggregation region of coarse particles.
4. The separation sharpness could be increased with an appropriate enlargement of the secondary-cylindrical section diameter to strengthen the particle circulation flow, whereas an excessively secondary-cylindrical section diameter will reduce the separation sharpness.

Supplementary Materials: The following supporting information can be downloaded at: https://www.mdpi.com/article/10.3390/pr11092542/s1, The numerical model, simulation conditions, and model applications are discussed in detail in the Supplementary Materials, while the particle circulation flow evaluation methods and calculation formulas are described in detail. Ref. [17] is cited in Supplementary Materials.

Author Contributions: Methodology, P.L. and B.C.; Software, D.H.; Validation, P.L. and Q.Z.; Formal analysis, D.H.; Resources, L.J.; Writing—original draft, D.H. and Q.Z.; Supervision, P.L. and D.W.; Project administration, D.W.; Funding acquisition, L.J. and B.C. All authors have read and agreed to the published version of the manuscript.

Funding: This work was funded by the National Natural Science Foundation of China [51974066, 52174244, and 22108159], the Open Foundation of State Key Laboratory of Mineral Processing [BGRIMM-KZSKL-2018-12], and the Natural Science Foundation of Shandong province, China [ZR2021QB068].

Data Availability Statement: No new data were created.

Conflicts of Interest: The authors declare no conflict of interest.

References

1. Svarovsky, L. *Hydrocyclones*; Holt Rinehart and Winston: London, UK, 1984.
2. Frachon, M.; Cilliers, J.J. A general model for hydrocyclone partition curves. *Chem. Eng. J.* **1999**, *73*, 53–59. [CrossRef]
3. Nunes, S.A.; Magalhaes, H.L.F.; Gomez, R.S.; Vilela, A.F.; Figueiredo, M.J.; Santos, R.S.; Rolim, F.D.; Souza, R.A.A.; Farias Neto, S.R.; Lima, A.G.B. Oily Water Separation Process Using Hydrocyclone of Porous Membrane Wall: A Numerical Investigation. *Membranes* **2021**, *11*, 79. [CrossRef] [PubMed]
4. Khatri, N.; Khatri, K.K.; Sharma, A. Enhanced Energy Saving in Wastewater Treatment Plant using Dissolved Oxygen Control and Hydrocyclone. *Environ. Technol. Innov.* **2020**, *18*, 100678. [CrossRef]
5. Padhi, M.; Mangadoddy, N.; Mainza, A.N.; Anand, M. Study on the particle interaction in a hydrocyclone classifier with multi-component feed blend at a high solids content. *Powder Technol.* **2021**, *393*, 380–396. [CrossRef]
6. Hou, D.X.; Cui, B.Y.; Zhang, H.; Zhao, Q.; Ji, A.K.; Wei, D.Z.; Feng, Y.Q. Designing the hydrocyclone with flat bottom structure for weakening bypass effect. *Powder Technol.* **2021**, *394*, 724–734. [CrossRef]
7. Zhang, Y.; Yang, M.; Jiang, L.; Wang, H.; Xu, J.; Yang, J. High Concentration Fine Particle Separation Performance in Hydrocyclones. *Minerals* **2021**, *11*, 307. [CrossRef]
8. Hao, M.X.; Zhang, Y.H.; Huang, Y.; Wang, H.L.; Li, H.; Du, J.-q.; Lv, W.-j.; Li, J.-p.; Fu, P.-b.; Wu, J.-w. Effect of particle self-rotation on separation efficiency in mini-hydrocyclones. *Powder Technol.* **2022**, *399*, 117165. [CrossRef]
9. Yang, Q.; Lv, W.J.; Ma, L.; Wang, H.L. CFD study on separation enhancement of mini-hydrocyclone by particulate arrangement. *Sep. Purif. Technol.* **2013**, *102*, 15–25. [CrossRef]

10. Wang, Z.-B.; Chu, L.-Y.; Chen, W.-M.; Wang, S.-G. Experimental investigation of the motion trajectory of solid particles inside the hydrocyclone by a Lagrange method. *Chem. Eng. J.* **2008**, *138*, 1–9. [CrossRef]
11. Fu, P.B.; Yu, H.; Li, Q.Q.; Cheng, T.T.; Zhang, F.Z.; Huang, Y.; Lv, W.; Xiu, G.; Wang, H. CFD-DEM simulation of particle revolution and high-speed self-rotation in cyclones with different structural and operating parameters. *Chem. Eng. J. Adv.* **2021**, *8*, 100176. [CrossRef]
12. Zhang, C.E.; Wei, D.Z.; Cui, B.Y.; Li, T.S.; Luo, N. Effects of curvature radius on separation behaviors of the hydrocyclone with a tangent-circle inlet. *Powder Technol.* **2017**, *305*, 156–165. [CrossRef]
13. Li, F.; Liu, P.K.; Yang, X.H.; Zhang, Y.K. Numerical simulation on the effects of different inlet pipe structures on the flow field and seperation performance in a hydrocyclone. *Powder Technol.* **2020**, *373*, 254–266. [CrossRef]
14. Kelsall, D.F. A study of the motion of solid particles in a hydraulic cyclone. *Trans. Inst. Chem. Eng.* **1952**, *30*, 87–104.
15. He, F.Q.; Zhang, Y.H.; Wang, J.G.; Yang, Q.; Wang, H.L.; Tan, Y.H. Flow Patterns in Mini-Hydrocyclones with Different Vortex Finder Depths. *Chem. Eng. Technol.* **2013**, *36*, 1935–1942. [CrossRef]
16. Hwang, K.J.; Hwang, Y.W.; Yoshida, H. Design of novel hydrocyclone for improving fine particle separation using computational fluid dynamics. *Chem. Eng. Sci.* **2013**, *85*, 62–68. [CrossRef]
17. Zhao, Q.; Cui, B.Y.; Wei, D.Z.; Song, T.; Feng, Y.Q. Numerical analysis of the flow field and separation performance in hydrocyclones with different vortex finder wall thickness. *Powder Technol.* **2019**, *345*, 478–491. [CrossRef]
18. Jiang, L.Y.; Liu, P.K.; Yang, X.H.; Zhang, Y.K. Short-Circuit Flow in Hydrocyclones with Arc-Shaped Vortex Finders. *Chem. Eng. Technol.* **2018**, *41*, 1783–1792. [CrossRef]
19. Hsu, C.Y.; Wu, R.M. Hot Zone in a Hydrocyclone for Particles Escape from Overflow. *Dry. Technol.* **2008**, *26*, 1011–1017. [CrossRef]
20. Liu, Y.; Yang, Q.; Qian, P.; Wang, H.L. Experimental study of circulation flow in a light dispersion hydrocyclone. *Sep. Purif. Technol.* **2014**, *137*, 66–73. [CrossRef]
21. Radman, J.R.; Langlois, R.; Leadbeater, T.; Finch, J.; Rowson, N.; Waters, K. Particle flow visualization in quartz slurry inside a hydrocyclone using the positron emission particle tracking technique. *Miner. Eng.* **2014**, *62*, 142–145. [CrossRef]
22. Vakamalla, T.R.; Vadlakonda, B.; Aketi, V.A.K.; Mangadoddy, N. Multiphase CFD Modelling of Mineral Separators Performance: Validation Against Tomography Data. *Trans. Indian Inst. Met.* **2016**, *70*, 323–340. [CrossRef]
23. Song, T.; Tian, J.Y.; Ni, L.; Shen, C.; Yao, Y. Experimental study on liquid flow fields in de-foulant hydrocyclones with reflux ejector using particle image velocimetry. *Sep. Purif. Technol.* **2020**, *240*, 116555. [CrossRef]
24. Huang, Y.; Wang, H.L.; Tian, J.Y.; Li, J.P.; Fu, P.B.; He, F.Q. Theoretical study on centrifugal coupling characteristics of self-rotation and revolution of particles in hydrocyclones. *Sep. Purif. Technol.* **2020**, *244*, 116552. [CrossRef]
25. Al Kayed Quteishat, M. Hydrocyclone flow characteristics and measurements. *Flow Meas. Instrum.* **2020**, *73*, 101741. [CrossRef]
26. Narasimha, M.; Brennan, M.; Holtham, P.N. A Review of CFD Modelling for Performance Predictions of Hydrocyclone. *Eng. Appl. Comput. Fluid Mech.* **2014**, *1*, 109–125. [CrossRef]
27. Tang, B.; Xu, Y.X.; Song, X.F.; Sun, Z.; Yu, J.G. Numerical study on the relationship between high sharpness and configurations of the vortex finder of a hydrocyclone by central composite design. *Chem. Eng. J.* **2015**, *278*, 504–516. [CrossRef]
28. Mokni, I.; Dhaouadi, H.; Bournot, P.; Mhiri, H. Numerical investigation of the effect of the cylindrical height on separation performances of uniflow hydrocyclone. *Chem. Eng. Sci.* **2015**, *122*, 500–513. [CrossRef]
29. Tian, J.Y.; Ni, L.; Song, T.; Shen, C.; Zhao, J.N. Numerical study of foulant-water separation using hydrocyclones enhanced by ejection device: Effect of ejection velocity. *Energy* **2018**, *163*, 641–659. [CrossRef]
30. Zhao, Q.; Cui, B.Y.; Wei, D.Z.; Feng, Y.Q.; He, Y.; Bayly, A.E. Linking separation sharpness with the characteristics of axial velocity wave zone in a hydrocyclone. *Powder Technol.* **2021**, *386*, 467–482. [CrossRef]
31. Tian, J.Y.; Ni, L.; Song, T.; Shen, C.; Yao, Y.; Zhao, J.N. Numerical study of foulant-water separation using hydrocyclones enhanced by reflux device: Effect of underflow pipe diameter. *Sep. Purif. Technol.* **2019**, *215*, 10–24. [CrossRef]
32. Hou, D.X.; Cui, B.Y.; Zhao, Q.; Wei, D.Z.; Song, Z.G.; Feng, Y.Q. Research on the structure of the cylindrical hydrocyclone spigot to mitigate the misplacement of particles. *Powder Technol.* **2021**, *387*, 61–71. [CrossRef]
33. Li, A.J.; Zhu, L.Y.; Wang, K.; Wang, G.T.; Wang, Z.B. Particles residence time distribution in a gas-solid cyclone reactor using a CFD-DDPM tracer method. *Powder Technol.* **2020**, *364*, 205–217. [CrossRef]
34. Hwang, I.S.; Jeong, H.J.; Hwang, J. Effects of vortex finder length on flow field and collection efficiency of cyclone in an industrial-scale circulating fluidized bed boiler: Numerical study. *Int. J. Energy Res.* **2020**, *44*, 7229–7241. [CrossRef]
35. Tian, J.Y.; Ni, L.; Song, T.; Zhao, J.N. CFD simulation of hydrocyclone-separation performance influenced by reflux device and different vortex-finder lengths. *Sep. Purif. Technol.* **2020**, *233*, 116013. [CrossRef]
36. Zhao, Q.; Hou, D.X.; Cui, B.Y.; Wei, D.Z.; Song, T.; Feng, Y.Q. Development of an integrated multichannel inlet for improved particle classification in hydrocyclones. *Adv. Powder Technol.* **2021**, *32*, 4546–4561. [CrossRef]
37. Hwang, I.S.; Jeong, H.J.; Hwang, J. Numerical simulation of a dense flow cyclone using the kinetic theory of granular flow in a dense discrete phase model. *Powder Technol.* **2019**, *356*, 129–138. [CrossRef]
38. Mousavian, S.M.; Najafi, A.F. Numerical simulations of gas–liquid–solid flows in a hydrocyclone separator. *Arch. Appl. Mech.* **2008**, *79*, 395–409. [CrossRef]
39. Vieira, L.G.M.; Silvério, B.C.; Damasceno, J.J.R.; Barrozo, M.A.S. Performance of hydrocyclones with different geometries. *Can. J. Chem. Eng.* **2011**, *89*, 655–662. [CrossRef]

40. Lim, E.W.C.; Chen, Y.-R.; Wang, C.-H.; Wu, R.-M. Experimental and computational studies of multiphase hydrodynamics in a hydrocyclone separator system. *Chem. Eng. Sci.* **2010**, *65*, 6415–6424. [CrossRef]
41. Narasimha, M.; Brennan, M.; Holtham, P.N. Large eddy simulation of hydrocyclone—Prediction of air-core diameter and shape. *Int. J. Miner. Process.* **2006**, *80*, 1–14. [CrossRef]
42. Hou, D.; Zhao, Q.; Cui, B.; Wei, D.; Song, Z.; Feng, Y. Geometrical configuration of hydrocyclone for improving the separation performance. *Adv. Powder Technol.* **2022**, *33*, 103419. [CrossRef]
43. Abbasi Moud, A.; Piette, J.; Danesh, M.; Georgiou, G.C.; Hatzikiriakos, S.G. Apparent slip in colloidal suspensions. *J. Rheol.* **2022**, *66*, 79–90. [CrossRef]
44. Abbasi Moud, A.; Poisson, J.; Hudson, Z.M.; Hatzikiriakos, S.G. Yield stress and wall slip of kaolinite networks. *Phys. Fluids* **2021**, *33*, 053105. [CrossRef]